

## ANALYSIS OF THREE-DIMENSIONAL STRUCTURES IN COMPLEX TURBULENT FLOWS

N. A. Fomin

UDC 681.327.12.001.362:525

The basic integral relations used in analyzing various images of flows are given. The differences in the Abel transform for laminar and turbulent flows have been shown. The integral Uberoi-Kovasznay transform used in analyzing direct-shadow images of turbulent flows has been described. The present possibilities of digital laser speckle-photography for analyzing speckle-images of turbulent flows with the use of integral Erbeck-Merzkirch transforms have been analyzed.

**Keywords:** Abel integral, turbulence, tomography, speckle-photography, correlation analysis.

**Introduction.** One of the most popular classes of optical methods of investigation of flows is the class of so-called "transillumination" methods in which the probing radiation is transmitted through the entire volume of the investigated inhomogeneity. Among them are:

- a) all kinds of interferometry, including reference beam interferometry, shearing, holographic, Talbot, and speckle interferometry [1];
- b) the whole spectrum of shadow methods, from color-shadow methods to speckle interferometry [2];
- c) probing of the investigated medium with the use of various laser sources, including spectrographs [3], etc.

Many of these methods are also referred to as the *flow visualization* technique, which underscores the qualitative character of diagnostics "by transillumination" rather than the quantitative one [1]. The main difficulty of quantitative interpretation of data therewith is the interpretation of the obtained information on the entire optical path of the probing radiation. For two-dimensional laminar flows, methods for quantitative processing of integral data with the use of the Abel transform have been developed [4–6]. Note that even for such flows the solution of the inverse Abel transform belongs to the class of ill-posed problems of mathematical physics.

Despite the fact that mathematical methods for solving such problems have been developed fairly well, in the quantitative interpretation of optical images obtained "by transillumination" the solution instability calls for a higher accuracy of recording primary experimental data, determining the urgent needs of digital (electrical) recording of images obtained [6, 7]. The difficulties of quantitative interpretation of data grow immeasurably in analyzing turbulent flows. For instance, the integral of the optical disturbance along the optical path will incorporate the fluctuating component

$$\Delta n = \frac{1}{L} \int_0^L (\langle n \rangle - n_\infty) ds + \frac{1}{L} \int_0^L n' ds .$$

This fact determines the main difficulties of quantitative interpretation of images "by transillumination" on going to the analysis of turbulent flows.

**Integral Abel Transform.** Consider a particular case of laser probing of an axisymmetric medium whose parameters at each point are described by the function  $f(r)$  (see Fig. 1).

Write the probing result in the form

$$F(y) = \int_{-\infty}^{\infty} f(r) dx .$$

---

A. V. Luikov Heat and Mass Transfer Institute, National Academy of Sciences of Belarus, 15 P. Brovka Str., Minsk, 220072, Belarus; email: fomin@hmti.ac.by. Translated from Inzhenerno-Fizicheskii Zhurnal, Vol. 82, No. 1, pp. 8–17, January–February, 2009. Original article submitted March 11, 2008.

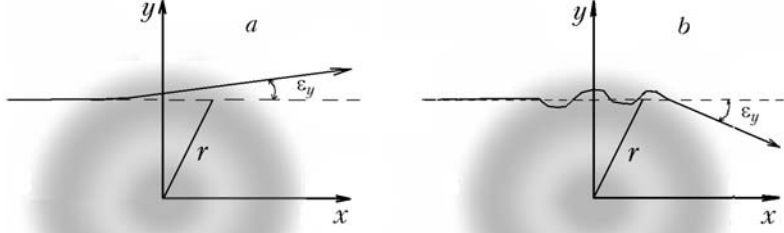


Fig. 1. Geometry of the laser probing of an axisymmetric object in recording the angles of deviation of the probing radiation: a) laminar flow, b) turbulent flow.

Replacing  $dx = 2rdr\sqrt{r^2 - y^2}$ , we obtain the relation between the functions  $F(y)$  and  $f(r)$  in terms of the standard Abel transform

$$F(y) = A\{f(x)\} = 2 \int_y^\infty \frac{f(r) r dr}{\sqrt{r^2 - y^2}},$$

which admits the inversion

$$f(r) = A^{-1}\{F(y)\} = -\frac{1}{\pi} \int_r^\infty \frac{dF}{dy} \frac{dy}{\sqrt{y^2 - r^2}}.$$

In recording the angle of deviation in the first approximation, for small angles of deviation we can assume  $\varepsilon_y(r) = \frac{\partial}{\partial y} \left[ \frac{n}{n_\infty} \right](r)$ :

$$\frac{\varepsilon_y(y)}{y} = 2 \int_y^\infty \frac{\partial}{\partial r} \left[ \frac{n}{n_\infty} \right] \frac{dr}{\sqrt{r^2 - y^2}} = A^{-1} \left\{ \left[ \frac{n}{n_\infty} \right](r) \right\}.$$

The inversion of this transform is of the form

$$n(r) = -\frac{n_\infty}{\pi} \int_r^\infty \frac{\varepsilon_y(y) dy}{\sqrt{y^2 - r^2}} = n_\infty A \left\{ \frac{\varepsilon_y(y)}{y} \right\}.$$

Taking account of the inevitable experimental errors, we replace the integral Abel transform by its estimate

$$\tilde{n}(r) = -\frac{n_\infty}{\pi} \int_r^\infty \frac{(\varepsilon_y(y) + \sigma_\varepsilon) dy}{\sqrt{y^2 - r^2}} = n_\infty \tilde{A} \left\{ \frac{\varepsilon_y(y) + \sigma_\varepsilon}{y} \right\}.$$

Such a form of writing reflects, in part, the influence of turbulent pulsations on the integral of the optical path, but provides no possibilities for obtaining quantitative information on the laws of turbulence. Examples of successful restructuring of the temperature fields in laminar axisymmetric flows can be found in a number of works using various optical methods [1, 2, 4–10].

**Uberoi and Kovaszny Approximation.** One of the first works in which an attempt at quantitative processing of direct-shadow images of turbulent flows was made is publication [11]. In this work, collimated radiation from

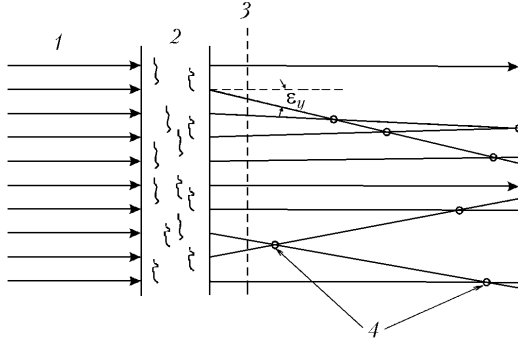


Fig. 2. Geometry of obtaining direct-shadow images in experiments of Uberoi and Kovazhnay [11]: 1) probing radiation; 2) turbulent flow; 3) plane of observation of the shadow pattern; 4) focusing caustics of the probing radiation on small-scale turbulent pulsations.

a flash lamp [12] was directed onto a plane turbulent flow and the direct-shadow picture was recorded in the near-field diffraction region lying before the first caustics of quasi-lenses formed by small-scale turbulent pulsations (see Fig. 2). The aim of shadow picture processing was to construct a two-dimensional correlation function of the optical density field (blackening) on the image plane with a three-dimensional correlation density function in the investigated turbulent flow. Determining, as in considering the Abel integral, the coordinate  $x$  along the direction of the probing radiation beams, we shall describe the image plane by coordinates  $(y', z')$  and the flow region by coordinates  $(x, y, z)$ .

For the isotropic field, the correlation density function will have the form

$$\mathcal{R}_\rho(\Delta r) = \langle \rho(r) \cdot \rho(r + \Delta r) \rangle = \langle \rho(x, y, z) \cdot \rho(x + \Delta x, y + \Delta y, z + \Delta z) \rangle .$$

Likewise, we define also the correlation functions of fluctuations of the refractive index in the turbulent flow

$$\mathcal{R}_n(\Delta r) = \langle n(r) \cdot n(r + \Delta r) \rangle = \langle n(x, y, z) \cdot n(x + \Delta x, y + \Delta y, z + \Delta z) \rangle .$$

The blackening density of the image of the direct-shadow picture  $T(y, z)$  is proportional to the integrals along the optical path of the second spatial derivatives of the density in the investigated turbulent flow

$$T(y', z') = \frac{LK}{\rho_\infty} \int_0^L \left( \frac{\partial^2}{\partial y^2} + \frac{\partial^2}{\partial z^2} \right) \rho(x, y, z) dx .$$

Accordingly, we seek the correlation function of the image optical density in the form

$$\mathcal{R}_T(\Delta y', \Delta z') = \langle T(y', z') \cdot T(y' + \Delta y', z' + \Delta z') \rangle = \langle T(y', z') \cdot T(y'_1, z'_1) \rangle ,$$

where the coordinates  $y'_1 = y' + \Delta y'$ ,  $z'_1 = z' + \Delta z'$ . With this notation

$$\mathcal{R}_T = \left\langle \left( \frac{LK}{\rho_\infty} \right)^2 \int_0^L \int_0^L \left( \frac{\partial^2}{\partial y^2} + \frac{\partial^2}{\partial z^2} \right) \left( \frac{\partial^2}{\partial y_1^2} + \frac{\partial^2}{\partial z_1^2} \right) \rho(x, y, z) \cdot \rho(x_1, y_1, z_1) dx dx_1 \right\rangle .$$

As a result of complicated manipulations and a number of simplifying assumptions, Uberoi and Kovasznay obtained the relation

$$\mathcal{R}_\rho(r) = \frac{1}{8\pi L} \left( \frac{\rho_\infty}{KL} \right)_r^\infty \mathcal{R}_T(\tau) \left[ \tau \frac{2r^2 + \tau^2}{r} \cos^{-1} \left| \frac{r}{\tau} \right| - 3\tau (\tau^2 - r^2)^{1/2} \right] d\tau .$$

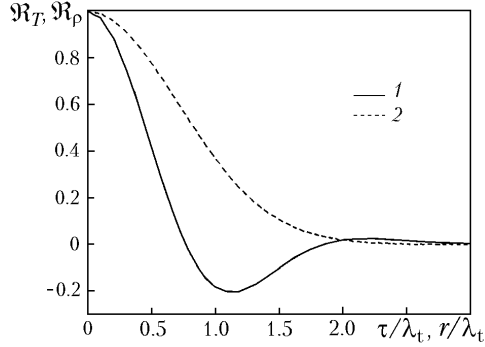


Fig. 3. Normalized Gaussian correlation functions of the direct-shadow image (1) and density (2) in the turbulent flow.

Let us write this transform in the symbolic form

$$\mathcal{R}_p(r) = \text{UK} \left\{ \mathcal{R}_T(\tau) \right\},$$

where UK is the integral Uberoi–Kovasznay transform.\* Here  $r^2 = x^2 + y^2 + z^2$ ;  $\tau^2 = (y')^2 + (z')^2$ .

Thus, as in the case of the laminar axisymmetric flow, the reconstruction of the three-dimensional correlation density function by the experimentally measured two-dimensional density function of the image reduces to the calculation of the inverse integral transform and belongs to the class of ill-posed problems of mathematical physics. Probably, exactly this fact impeded the use of the integral Uberoi–Kovasznay transform for many years — until the advent of digital imaging systems. Calculations are considerably simplified in defining the form of the correlation functions. For instance, if the three-dimensional correlation density function is represented in the Gaussian form with one microscale of density fluctuations in the turbulent flows as  $\frac{\mathcal{R}_p(r)}{\mathcal{R}_p(0)} = \exp \left( -\frac{r}{\lambda_{tp}} \right)$ , then the correlation function of the

image in the first approximation will be written as follows:  $\frac{\mathcal{R}_T(\tau)}{\mathcal{R}_T(0)} = \left[ 1 - 2 \left( \frac{\tau}{\lambda_{tp}} \right)^2 + \frac{1}{2} \left( \frac{\tau}{\lambda_{tp}} \right)^4 \right] \exp \left[ -\frac{\tau}{\lambda_{tp}} \right]$ . In so doing,

the whole procedure of quantitative image processing is reduced to the determination of one unknown — the microscale of turbulence  $\lambda_t$ . Figure 3 illustrates the different character of the behavior of correlation functions at such an approximation. Small-scale turbulence in the experiment of [11] was created in a layer of mixing of seven transonic jets flowing through a projectile with large holes called by the authors "Swiss cheese." The scales of turbulent flow

were determined by the correlation function of image blackening: for macroscale  $\Lambda_{tp} = \int_0^\infty \frac{\mathcal{R}_T(\tau)d\tau}{\mathcal{R}_T(0)}$ ; for microscale  $\lambda_{tp}^2 =$

$-2 \frac{\mathcal{R}_T(0)}{\mathcal{R}_T''(0)}$ . For the microscale of turbulence the estimate  $\lambda_{tp} = 300 \mu\text{m}$  was obtained. Using the dependence  $2\lambda_{tp}^2/\lambda_U^2 =$

$= \text{Pr}$  and assuming the value of the Prandtl number for air 0.7, we estimate the microscale of turbulent pulsations of velocity as  $\lambda_U = \lambda_{tp} = 180 \mu\text{m}$ . For comparison with thermoanemometric data, additional experiments were performed. In this case, small-scale turbulence was created in a free jet flowing around a nichrome net with a diameter of fibers 0.8 mm spaced at 6.2 mm. In this case, the microscale of turbulence, according to the analysis of the direct-shadow picture, was  $\lambda_{tp} = 1.45 \text{ mm}$ , and according to the thermoanemometric data it was equal to 1.23 mm. Note that the microscale of turbulence reconstructed upon integration of the spectral distribution of temperature pulsations obtained from the thermoanemometric data equaled 8.5 mm.

---

\*In the original work of Uberoi and Kovasznay [11], this integral transform is classified as a Fourier–Bessel transform with reference to the hardly available Kovasznay work of 1949 [13].

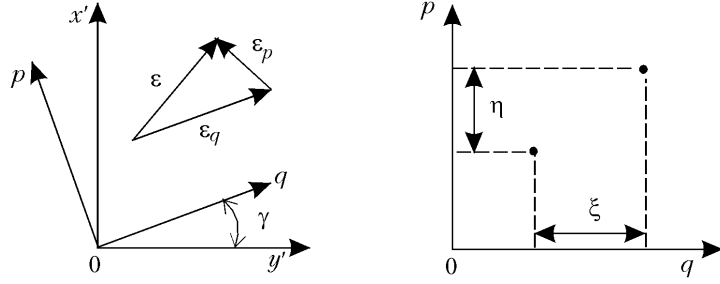


Fig. 4. Coordinate systems for calculating the correlation functions of the angles of deviation of the probing radiation.

Thus, the early experiments conducted by Uberoi and Kovasznay [11] have shown that in principle quantitative interpretation of optical images for turbulent flows is possible. The integral transform obtained and used in this work places stringent requirements upon the accuracy of optical data processing. Analogous approaches are also fully realized at present in digital processing of obtained images.

**Erbeck–Merzkirch Integral Transform.** Following the methodology of Uberoi and Kovasznay, Erbeck and Merzkirch established the relation between the two-dimensional correlation functions of angles of deviation of the probing radiation and the three-dimensional density function in a turbulent flow [14]. The angles of deviation were determined, in deriving these relations, by solving the eikonal equation [7]

$$\frac{d}{ds} \left( n \frac{dr}{ds} \right) = \text{grad}(n)$$

and its equivalent system of Weyl differential equations [15]

$$\begin{aligned} \frac{d^2x}{dz^2} &= \left\{ 1 + \left( \frac{dx}{dz} \right)^2 + \left( \frac{dy}{dz} \right)^2 \right\} \left\{ \frac{\partial n}{n \partial x} + \frac{dx}{dz} \frac{\partial n}{n \partial z}^2 \right\}, \\ \frac{d^2y}{dz^2} &= \left\{ 1 + \left( \frac{dx}{dz} \right)^2 + \left( \frac{dy}{dz} \right)^2 \right\} \left\{ \frac{\partial n}{n \partial y} + \frac{dy}{dz} \frac{\partial n}{n \partial z}^2 \right\}. \end{aligned}$$

The angle of deviation of the probing radiation can be given by a vector on the observation plane ( $y'$ ,  $z'$ ) or in a system of "digital" coordinates ( $p$ ,  $q$ ) which can be turned by angle  $\gamma$  with respect to ( $y'$ ,  $z'$ ), as is shown in Fig. 4:

$$\boldsymbol{\epsilon}(y', z') = \epsilon_y \mathbf{i}' + \epsilon_z \mathbf{j}' = \epsilon_p \mathbf{i} + \epsilon_q \mathbf{j}.$$

Here ( $p$ ) and ( $q$ ) are counted in pixels. Let us write the correlation functions in this coordinate system:

$$\mathcal{R}_{\epsilon_p}(\Delta\tau) = \langle \epsilon_p(\tau) \cdot \epsilon_p(\tau + \Delta\tau) \rangle = \langle \epsilon_p(p, q) \cdot \epsilon_p(p + \Delta p, q + \Delta q) \rangle,$$

$$\mathcal{R}_{\epsilon_q}(\Delta\tau) = \langle \epsilon_q(\tau) \cdot \epsilon_q(\tau + \Delta\tau) \rangle = \langle \epsilon_q(p, q) \cdot \epsilon_q(p + \Delta p, q + \Delta q) \rangle.$$

The parallel and perpendicular correlation functions are defined as follows:

$$\mathcal{R}_{\epsilon_{p\perp}}(\Delta\tau) = \langle \epsilon_p(p, q) \cdot \epsilon_p(p, q + \Delta q) \rangle, \quad \mathcal{R}_{\epsilon_{p\parallel}}(\Delta\tau) = \langle \epsilon_p(p, q) \cdot \epsilon_p(p + \Delta p, q) \rangle,$$

$$\mathcal{R}_{\epsilon_{q\perp}}(\Delta\tau) = \langle \epsilon_q(p, q) \cdot \epsilon_q(p + \Delta p, q) \rangle, \quad \mathcal{R}_{\epsilon_{q\parallel}}(\Delta\tau) = \langle \epsilon_q(p, q) \cdot \epsilon_q(p, q + \Delta q) \rangle.$$

In digital recording of angles of deviation by means of a CCD matrix, the coordinates ( $p$ ,  $q$ ) can be interpreted as integers defining the pixel number in the matrix along the corresponding coordinate. In this case, the correlation functions can be calculated by summing up the series

$$\mathcal{R}_{\epsilon_p^\perp}(\Delta\tau) = \mathcal{R}_{\epsilon_p^\perp}(\Delta q) = \frac{1}{M - \Delta q} \sum_{\Delta q=1}^{M-\Delta q} \langle \epsilon_p(p, q) \cdot \epsilon_p(p, q + \Delta q) \rangle ,$$

$$\mathcal{R}_{\epsilon_p^\parallel}(\Delta\tau) = \mathcal{R}_{\epsilon_p^\parallel}(\Delta p) = \frac{1}{M - \Delta p} \sum_{\Delta p=1}^{M-\Delta p} \langle \epsilon_p(p, q) \cdot \epsilon_p(p + \Delta p, q) \rangle ,$$

$$\mathcal{R}_{\epsilon_q^\parallel}(\Delta\tau) = \mathcal{R}_{\epsilon_q^\parallel}(\Delta q) = \frac{1}{M - \Delta q} \sum_{\Delta q=1}^{M-\Delta q} \langle \epsilon_q(p, q) \cdot \epsilon_q(p, q + \Delta q) \rangle ,$$

$$\mathcal{R}_{\epsilon_q^\perp}(\Delta\tau) = \mathcal{R}_{\epsilon_q^\perp}(\Delta p) = \frac{1}{M - \Delta p} \sum_{\Delta p=1}^{M-\Delta p} \langle \epsilon_q(p, q) \cdot \epsilon_q(p + \Delta p, q) \rangle .$$

In this coordinate system, the correlation density function will still be scalar

$$\mathcal{R}_\rho(\Delta r) = \langle \rho(r) \cdot \rho(r + \Delta r) \rangle = \langle \rho(p, q, s) \cdot \rho(p + \Delta p, q + \Delta q, s + \Delta s) \rangle$$

and can be calculated by summing up the series

$$\mathcal{R}_\rho(\Delta r) = \frac{1}{(M - \Delta p)(M - \Delta q)(M - \Delta s)} \sum_{\Delta p=1}^{M-\Delta p} \sum_{\Delta q=1}^{M-\Delta q} \sum_{\Delta s=1}^{M-\Delta s} \rho(p, q, s) \cdot \rho(p + \Delta p, q + \Delta q, s + \Delta s) .$$

One can distinguish three scalar components of this function

$$\mathcal{R}_\rho(\Delta p) = \frac{1}{M - \Delta p} \sum_{\Delta p=1}^{M-\Delta p} \rho(p, q, s) \cdot \rho(p + \Delta p, q, s) ,$$

$$\mathcal{R}_\rho(\Delta q) = \frac{1}{M - \Delta q} \sum_{\Delta q=1}^{M-\Delta q} \rho(p, q, s) \cdot \rho(p, q + \Delta q, s) ,$$

$$\mathcal{R}_\rho(\Delta s) = \frac{1}{M - \Delta s} \sum_{\Delta s=1}^{M-\Delta s} \rho(p, q, s) \cdot \rho(p, q, s + \Delta s) .$$

Since

$$\epsilon_p = K \int_0^L \frac{\partial \rho(p, q, s)}{\partial p} ds , \quad \epsilon_q = K \int_0^L \frac{\partial \rho(p, q, s)}{\partial q} ds ,$$

the correlation functions for the angles of deviation of the probing radiation will be written in the form

$$\mathcal{R}_{\epsilon_p}(\Delta p, \Delta q) = \left\langle K \int_0^L \frac{\partial \rho(p, q, s)}{\partial p} ds \cdot K \int_0^L \frac{\partial \rho(p + \Delta p, q + \Delta q, s)}{\partial p} ds \right\rangle ,$$

$$\mathcal{R}_{\epsilon_q}(\Delta p, \Delta q) = \left\langle K \int_0^L \frac{\partial \rho(p, q, s)}{\partial q} ds \cdot K \int_0^L \frac{\partial \rho(p + \Delta p, q + \Delta q, s)}{\partial q} ds \right\rangle .$$

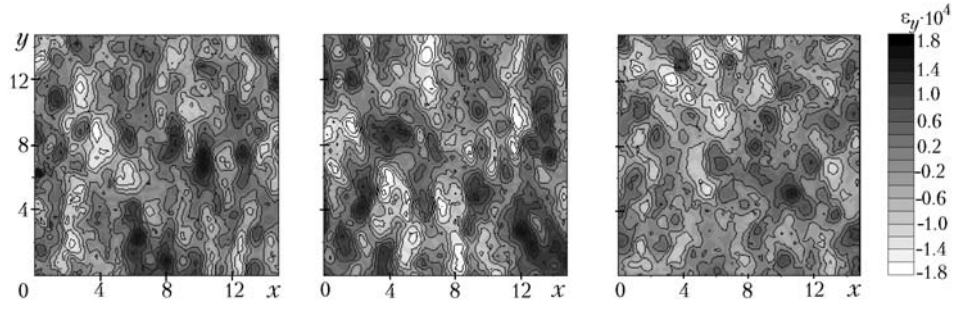


Fig. 5. Examples of isolines of the angles of deviation of the probing radiation reconstructed for various cross-sections of the turbulent flow by the method of digital laser speckle photography.

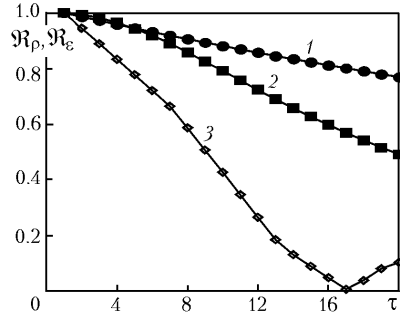


Fig. 6. Correlation functions of the density (1, 2) and the angles of deviation of the probing radiation (3) according to the data of direct numerical simulation of the laser radiation propagation through a turbulent medium.

Using these relations, Erbeck and Merzkirch obtained for isotropic turbulence the following integral transforms relating the three-dimensional correlation density function to the two-dimensional correlation function of the angles of deviation of the probing radiation:

$$\begin{aligned} \mathcal{R}_{\epsilon_p}(\tau) &= -2K^2 L \int_0^L \frac{\partial^2}{\partial \Delta p^2} \mathcal{R}_p(\sqrt{\tau^2 + \Delta s^2}) d\Delta s, \\ \mathcal{R}_{\epsilon_q}(\tau) &= -2K^2 L \int_0^L \frac{\partial^2}{\partial \Delta q^2} \mathcal{R}_p(\sqrt{\tau^2 + \Delta s^2}) d\Delta s. \end{aligned}$$

Note that these integral relations assume inversion by which the correlation density function can be reconstructed by the correlation functions of the angles of deviation of the probing radiation:

$$\begin{aligned} \mathcal{R}_p(r) &= \frac{1}{\pi K^2 L} \int_r^\infty \frac{1}{\sqrt{\tau^2 - r^2}} \left\{ \int_0^\tau \mathcal{R}_{\epsilon_p \parallel}(\tau^*) d\tau^* \right\} d\tau, \quad \mathcal{R}_p(r) = \frac{1}{\pi K^2 L} \int_r^\infty \frac{1}{\sqrt{\tau^2 - r^2}} \left\{ \int_0^\tau \mathcal{R}_{\epsilon_q \parallel}(\tau^*) d\tau^* \right\} d\tau, \\ \mathcal{R}_p(r) &= \frac{\tau}{\pi K^2 L} \int_r^\infty \frac{\mathcal{R}_{\epsilon_p \perp} d\tau}{\sqrt{\tau^2 - r^2}}, \quad \mathcal{R}_p(r) = \frac{\tau}{\pi K^2 L} \int_r^\infty \frac{\mathcal{R}_{\epsilon_q \perp} d\tau}{\sqrt{\tau^2 - r^2}}. \end{aligned}$$

Let us denote these integral Erbeck–Merzkirch relations for the sake of brevity similarly to the above Abel and Uberoi–Kovasznay relations:

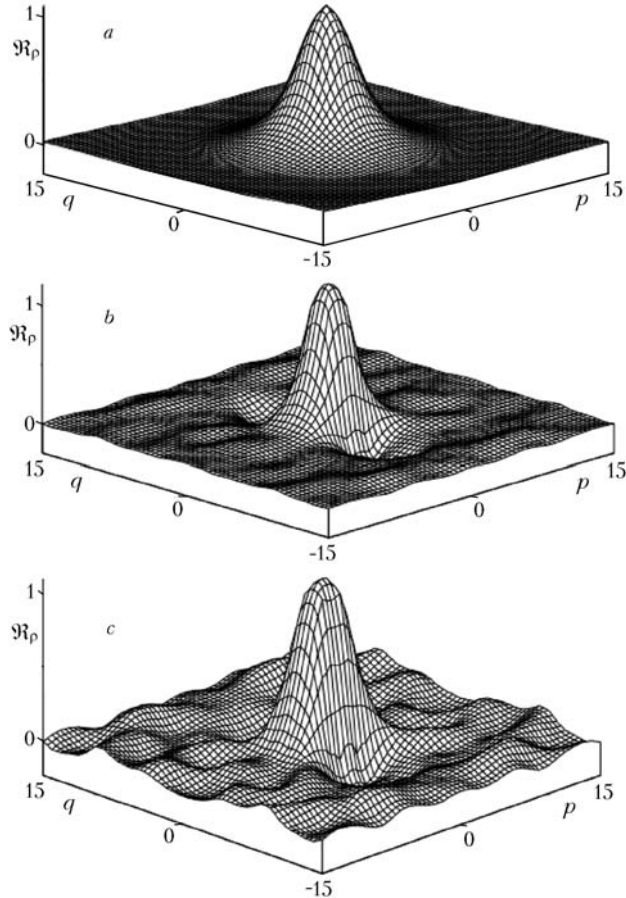


Fig. 7. Initial (phantom) correlation density function (a) and functions reconstructed with the use of the Erbeck–Merzkirch integral transform [b] without superposition of additional experimental noise, c) with superposition of 5% noise].

$$\mathcal{R}_p(r) = \text{EM} \left\{ \mathcal{R}_e(\tau) \right\}.$$

Note that the reconstruction of the three-dimensional correlation density function by the data on the distribution of angles of deviation of the probing radiation is, as before, an ill-posed problem of mathematical physics and, therefore, such a reconstruction requires a high accuracy of experimental data recording. As in using the integral Uberoi–Kovasznay transforms, in this case analytic relations for correlation functions in which Kolmogorov microscales of turbulence appear turn out to be useful. In using the Gauss law for the correlation density function  $\frac{\mathcal{R}_p(r)}{\mathcal{R}_p(0)} = \exp \left( -\frac{r}{\lambda_{tp}} \right)$ , the correlation functions for the angles of deviation of the probing radiation are defined as

$$\frac{\mathcal{R}_{e\perp}(\tau)}{\mathcal{R}_{e\perp}(0)} = \exp \left( -\left( \frac{\tau}{\lambda_{tp}} \right)^2 \right), \quad \frac{\mathcal{R}_{e\parallel}(r)}{\mathcal{R}_{e\parallel}(0)} = 1 + 2 \left[ \frac{\tau}{\lambda_{tp}} \right]^2 \exp \left[ -\left( \frac{\tau}{\lambda_{tp}} \right)^2 \right] - 4 \left[ \frac{\tau}{\lambda_{tp}} \right]^4 \exp \left[ -\left( \frac{\tau}{\lambda_{tp}} \right)^2 \right].$$

Figure 5 shows the isolines of the angles of deviation of the probing laser radiation for various turbulent flow cross-sections obtained in analyzing the digital speckle image [16]. The accuracy of reconstruction of the correlation function by such measurement data is illustrated in Fig. 6 according to the data of direct numerical simulation of the laser radiation propagation through a turbulent medium [17]. Comparison of curve 1 to the initial phantom distribution 2 points to a high accuracy of determination of microscales of turbulence, whereas in determining macroscales the er-

rors increase. The same tendency for an increase in the error in determining the macroscale of turbulence was also noted in the early experiments of Uberoi and Kovasznay.

Figure 7 illustrates the form of the initial correlation function (a) and of those reconstructed with the use of the "exact" data of direct numerical simulation (b) and upon superposition of random 5% errors on the experimental data in image processing (c). As is seem from these data, artefacts arise already upon superposition of small experimental errors. At the same time, the form of the correlation function near the origin of coordinates remains unaltered, which makes it possible to determine with a good accuracy the microscales of turbulence. A number of recent works [18, 19] have been devoted to the experimental illustration of this fact.

**Acknowledgements.** The author wishes to thank Prof. Wolfgang Merzkirch, Doctors of Sciences Ulrich Werneking, Ralf Erbeck, and Oleg Penyazkov, and Candidates of Sciences Nikolai Bazylev, Pavel Khramtsov, and Elena Lavinskaya for helpful discussions, recommendations, and assistance in conducting experiments and developing programs for mathematical treatment of images, as well as the Belarusian Republic Basic Research Foundation and the NAS of Belarus for supporting part of the work with grants and projects "Vodorod-19," "Nanotech 1.13," and "Teplovye Protsessy-25," T07-70, T07F-005.

## NOTATION

$A\{f(x)\}$ , integral Abel transform;  $A^{-1}\{F(y)\}$ , inverse integral Abel transform;  $\tilde{A}$ , estimate of the integral Abel transform;  $EM$ , integral Erbeck–Merzkirch transform;  $K$ , Gladstone–Dale constant,  $m^3/kg$ ;  $L$ , optical path of the probing radiation, m;  $M$ , number of pixels in the CCD matrix array;  $n$ , optical refractive index of the medium;  $Pr$ , Prandtl number;  $T(y, z)$ , optical density of the image;  $UK$ , integral Uberoi–Kovasznay transform;  $U$ , velocity,  $m/sec$ ;  $(x, y, z)$ ,  $(x', y', z')$  linear spatial coordinates, m;  $(p, q, s)$ , spatial coordinates on the CCD matrix in the image plane,  $py$ ;  $\mathbf{r}$ , radius vector in the physical region;  $\epsilon_y$ , angle of deviation of the probing radiation along the  $y$  axis as a result of refraction, rad;  $\lambda_t$ , Kolmogorov turbulence microscale, mm;  $\lambda_{tp}$  and  $\lambda_{tU}$ , Kolmogorov turbulence microscales calculated for the density and velocity, respectively, mm;  $\rho$ , density,  $kg/m^3$ ;  $\tau$ , radius vector in the image plane;  $\sigma_\epsilon$ , experimental error in determining the angle of deviation of the probing radiation;  $\mathfrak{R}_p(\Delta r)$ , autocorrelation density function in the turbulent flow;  $\mathfrak{R}_n(\Delta r)$ , autocorrelation function of the refractive index in the turbulent flow;  $\mathfrak{R}_T(\Delta y', \Delta z')$ , autocorrelation density function of the image in its plane;  $\mathfrak{R}_{\epsilon_p^\perp}$ , autocorrelation function of the  $p$ -component of the angle of deviation of the probing radiation calculated in the perpendicular direction;  $\mathfrak{R}_{\epsilon_p^\parallel}$ , autocorrelation function of the  $p$ -component of the angle of deviation of the probing radiation calculated in the longitudinal direction;  $\mathfrak{R}_{\epsilon_q^\parallel}$ , autocorrelation function of the  $q$ -component of the angle of deviation of the probing radiation calculated in the longitudinal direction;  $\mathfrak{R}_{\epsilon_q^\perp}$ , autocorrelation function of the  $q$ -component of the angle of deviation of the probing radiation calculated in the perpendicular direction. Subscripts:  $\infty$ , parameters in the undisturbed region;  $t$ , turbulence.

## REFERENCES

1. W. Merzkirch, *Flow Visualization*, 2nd. ed., Academic Press, Orlando (1987).
2. G. S. Settles, *Schlieren and Shadowgraph Techniques. Visualizing Phenomena in Transparent Media*, Springer Verlag, New York (2001).
3. O. V. Achasov, N. N. Kudryavtsev, S. S. Novikov, R. I. Soloukhin, and N. A. Fomin, *Diagnostics of Non-equilibrium States in Molecular Lasers* [in Russian], Nauka i Tekhnika, Minsk (1985).
4. H. Schardin, Die Schlierenverfahren und ihre Anwendungen, *Naturwissenschaft*, **20**, 303–439 (1949).
5. W. Hauf and U. Grigull, Optical methods in heat transfer, *Adv. Heat Transfer*, **6**, 131–366 (1970).
6. M. M. Skotnikov, *Quantitative Shadow Methods in Gas Dynamics* [in Russian], Nauka, Moscow (1976).
7. N. Fomin, *Speckle Photography for Fluid Mechanics Measurements*, Springer Verlag, Berlin (1998).
8. G. N. Blinkov, D. E. Vitkin, R. I. Soloukhin, and N. A. Fomin, Speckle photography of the local temperatures fields in the processes of heat and mass transfer with axial symmetry, *Dokl. Akad. Nauk BSSR*, **31**, No. 7, 627–630 (1987).
9. C. Shakher and A. K. Anil Kumar Nirala, A review on refractive index and temperature measurements using laser-based interferometric techniques, *Opt. Lasers Eng.*, **31**, 455–491 (1999).

10. M. V. Dorozhko, O. G. Penyazkov, G. Renkin, P. P. Khramtsov, and I. A. Shikh, Talbot interferometry in measurements of parameters of an axisymmetric turbulent jet, *Inzh.-Fiz. Zh.*, **79**, No. 5, 94–99 (2006).
11. M. S. Uberoi and L. S. G. Kovasznay, Analysis of turbulent density fluctuations by shadow method, *J. Appl. Phys.*, **26**, No. 1, 19–24 (1955).
12. L. S. G. Kovasznay, High power short duration spark discharge, *Rev. Sci. Instrum.*, **20**, 696–697 (1949).
13. L. S. G. Kovasznay, *Heat Transfer in Fluid Mechanics Institute*, American Society of Mechanical Engineers, Berkeley (1949).
14. R. Erbeck and W. Merzkirch, Speckle photographic measurement of turbulence in an air stream with fluctuation temperature, *Exp. Fluids*, **6**, 89–93 (1988).
15. F. J. Weyl, Analysis of optical methods, in: *Physical Measurements in Gas Dynamics and Combustion*, Princeton University Press, Princeton (1954), pp. 3–25.
16. D. Vitkin, W. Merzkirch, and N. Fomin, Quantitative visualization of the change of turbulence structure caused by a normal shock wave, *J. Visualiz.*, **1**, No. 1, 29–35 (1998).
17. E. I. Lavinskaya, E. F. Nogotov, and N. A. Fomin, Statistical analysis of turbulence from the data of speckle photography of the flow, *Dokl. Nats. Akad. Nauk Belarusi*, **41**, No. 4, 53–57 (1997).
18. N. Fomin, E. Lavinskaya, and K. Takayama, Limited projections laser speckle tomography of complex flows, *Opt. Lasers Eng.*, **44**, Nos. 3-4, 335–349 (2006).
19. N. A. Fomin, O. G. Penyazkov, P. P. Khramtsov, and E. I. Lavinskaya, 3D turbulence diagnostics by digital speckle photography and Talbot interferometry, in: *Proc. Int. Conf. on the Methods of Aerophysical Research ICMAR-2007*, Pt. IV, Publ. House "Parallel," Novosibirsk (2007), pp. 22–27.